Arabidopsis CHLI2 Can Substitute for CHLI1[1][C][W][OA]

Yi-Shiuan Huang and Hsou-min Li*

Graduate Institute of Life Sciences, National Defense Medical Center, Taipei 114, Taiwan (Y.-S.H.); and Institute of Molecular Biology, Academia Sinica, Taipei 115, Taiwan (Y.-S.H., H.-m.L.)

The I subunit of magnesium-chelatase (CHLI) is encoded by two genes in Arabidopsis (*Arabidopsis thaliana*), *CHLI1* and *CHLI2*. Conflicting results have been reported concerning the functions of the two proteins. We show here that the *chli1/chli1 chli2/chli2* double knockout mutant was albino. Comparison with the pale-green phenotype of a *chli1/chli1* single knockout mutant indicates that CHLI2 could support some chlorophyll biosynthesis in the complete absence of CHLI1. Real-time quantitative reverse transcription-polymerase chain reaction showed that *CHLI2* was expressed at a much lower level than *CHLI1*. The *chli1/chli1 chli2/chli2* double mutant could be fully rescued by expressing a transgene of *CHLI2* driven by the *CHLI1* promoter. These results suggest that differences between CHLI1 and CHLI2 lie mostly in their expression levels. Furthermore, both the *chli1/chli1* and *chli2/chli2* single knockout mutants had lower survival rates during de-etiolation than the wild type, suggesting that both genes are required for optimal growth during de-etiolation. In addition, we show that a semidominant *chli1* mutant allele and the *chli1/chli1 chli2/chli2* double mutant accumulated *Lhcb1* transcripts when treated with the herbicide norflurazon, indicating that knocking out the CHLI activity causes the *genome-uncoupled* phenotype.

Magnesium (Mg)-chelatase catalyzes the first committed step toward chlorophyll synthesis in the tetrapyrrole biosynthesis pathway. The enzyme inserts Mg^{2+} into protoporphyrin IX and produces Mg-protoporphyrin IX. The enzyme is composed of three subunits: CHLH, CHLD, and CHLI (corresponding to BchH, BchD, and BchI in *Rhodobacter* and XAN-F, XAN-G, and XAN-H in barley [*Hordeum vulgare*], respectively). Both in vitro and in vivo evidence has shown that all three subunits are essential for the Mg-chelatase activity (Gibson et al., 1995; Willows et al., 1996; Kannangara et al., 1997). The H subunit binds protoporphyrin IX and may be the catalytic subunit for the metallation reaction. The D and I subunits form an activation complex in an ATP- and Mg^{2+}-dependent manner. In Arabidopsis (*Arabidopsis thaliana*), both the D and H subunits are encoded by single genes.

CHLI belongs to the AAA^+ (ATPases associated with various cellular activities) family of ATPases. It forms a ring-shaped homohexamer. Many semidominant and recessive alleles of *chli* mutants have been isolated from various species (Kjemtrup et al., 1998; Fitzmaurice et al., 1999; Hansson et al., 2002; Soldatova et al., 2005). The semidominant alleles are all missense mutations that still produce full-length proteins. The mutant proteins can assemble with the wild-type proteins into the hexameric ring, hindering the ATPase activity and therefore resulting in the semidominant phenotype (Hansson et al., 2002).

CHLI isoforms in Arabidopsis are encoded by two genes: *CHLI1* (At4g18480) and *CHLI2* (At5g45930). CHLI1 seems to be the major functional form, since chlorophyll levels in *chli1*-null mutants are reduced to 10% to 17% of the wild-type level (Rissler et al., 2002). Some reports have shown that *CHLI1* and *CHLI2* RNAs are expressed at similar levels (Rissler et al., 2002; Apchelimov et al., 2007). Because CHLI2 protein was not detected even in isolated *chli1* mutant plastids, it has been proposed that CHLI2 is subjected to rapid posttranslational turnover and does not accumulate in vivo (Rissler et al., 2002). Alternatively, it has also been suggested that CHLI2 cannot assemble into the hexameric ring structure due to changes in residues in its C terminus (Apchelimov et al., 2007). However, from a miniarray experiment examining all genes involved in tetrapyrrole biosynthesis (Matsumoto et al., 2004) and also from the Genevestigator (https://www.genevestigator.ethz.ch/; Zimmermann et al., 2004) and MPSS (for Massively Parallel Signature Sequencing; http://mpss.udel.edu/at/; Brenner et al., 2000) databases, the expression level of *CHLI2* is shown to be much lower than that of *CHLI1*. It is possible, therefore, that CHLI2 function could not be observed due to its very low expression level. Indeed, it has been shown that recombinant CHLI2 has ATPase activity, although with a lower V_{max} and K_{mATP} than CHLI1 (Kobayashi et al., 2008). A double mutant of a

[1] This work was supported by the National Science Council (grant no. NSC–97–2321–B–001–001 to H.-m.L.) and the Academia Sinica of Taiwan.

* Corresponding author; e-mail mbhmli@gate.sinica.edu.tw.

The author responsible for distribution of materials integral to the findings presented in this article in accordance with the policy described in the Instructions for Authors (www.plantphysiol.org) is: Hsou-min Li (mbhmli@gate.sinica.edu.tw).

[C] Some figures in this article are displayed in color online but in black and white in the print edition.

[W] The online version of this article contains Web-only data.

[OA] Open Access articles can be viewed online without a subscription.

www.plantphysiol.org/cgi/doi/10.1104/pp.109.135368

partially functional light-green allele of *chli1*, *cs* (or *ch42-2*), with a *chli2*-knockout mutant, is albino. This result indicates that at least in the presence of a partially functional CHLI1, CHLI2 can contribute to some chlorophyll biosynthesis (Kobayashi et al., 2008).

The tetrapyrrole biosynthesis pathway also seems to be important for retrograde signaling from plastids to the nucleus. One frequently used method for studying the signaling pathway is to treat plants with the herbicide norflurazon (Nf), which inhibits carotenoid biosynthesis and causes photo-oxidative damage to plastids. This treatment results in repressed expression of nucleus-encoded photosynthetic genes like *Lhcb1* in response to signals sent by the damaged plastids. Arabidopsis mutants that still express *Lhcb1* in the presence of Nf have been identified and are named *genome uncoupled* (*gun*) mutants (Susek et al., 1993; Cottage et al., 2008). Noticeably, four of the original five *gun* mutants are defective in tetrapyrrole biosynthesis. The *gun2* and *gun3* mutants are defective in heme oxygenase and phytochromobilin synthase, respectively. The *gun5* mutant has a missense mutation in *CHLH*, and *GUN4* encodes a regulator of Mg-chelatase (Mochizuki et al., 2001; Larkin et al., 2003). A knockout mutation in *CHLD* also results in the *gun* phenotype (Strand et al., 2003). Therefore, it seems that perturbation of Mg-chelatase activity would result in the *gun* phenotype. However, two alleles of the *chli1* mutants, *ch42* (*ch42-1*) and *cs* (*ch42-2*), do not accumulate *Lhcb1* transcripts when treated with Nf and therefore are not *gun* mutants (Mochizuki et al., 2001). It has been proposed that the presence of *CHLI2* in the *chli1* mutants may be sufficient to allow functioning of the retrograde signaling pathway (Nott et al., 2006).

During our search for Arabidopsis mutants defective in protein import into chloroplasts, several pale-green or albino mutants were collected from various sources. One of the mutants from the Arabidopsis Biological Resource Center (ABRC), *cs215*, although not defective in protein import (data not shown), showed an interesting semidominant phenotype. Homozygous *cs215* mutants were albino, while heterozygous plants were pale green. Positional cloning of the *cs215* locus revealed that *cs215* is a new allele of *chli1* mutants. To compare *cs215* with other *chli* mutants, we obtained T-DNA or Ds insertion alleles of *chli1* and *chli2* mutants and generated various double mutants. Our results indicated that the low functionality of *CHLI2* was mostly due to its low expression level compared with that of *CHLI1*. We further tested the homozygous *cs215* mutant and the *chli1/chli1 chli2/chli2* double mutant for the *gun* phenotype. When treated with Nf, the *chli1/chli1 chli2/chli2* double mutant accumulated *Lhcb1* to a level similar to that observed in a *chld*-knockout mutant and the *cs215* homozygous mutant accumulated an even higher level of *Lhcb1*, similar to that observed in a *chlh*-knockout mutant, suggesting that knocking out the CHLI activity also caused the *gun* phenotype.

RESULTS

Identification of the *cs215* Locus

Homozygous *cs215* (*cs215/cs215*) mutants were albino, while heterozygous (*cs215/+*) plants were pale green (Fig. 1). To identify the *cs215* locus, we crossed the *cs215/+* mutant with Columbia (Col) and Landsberg erecta (L*er*) wild-type plants because the *cs215* mutant is in the ecotype Enkheim (Enk). We identified PCR-based polymorphic markers that distinguish between the Enk and Col/L*er* ecotypes (see "Materials

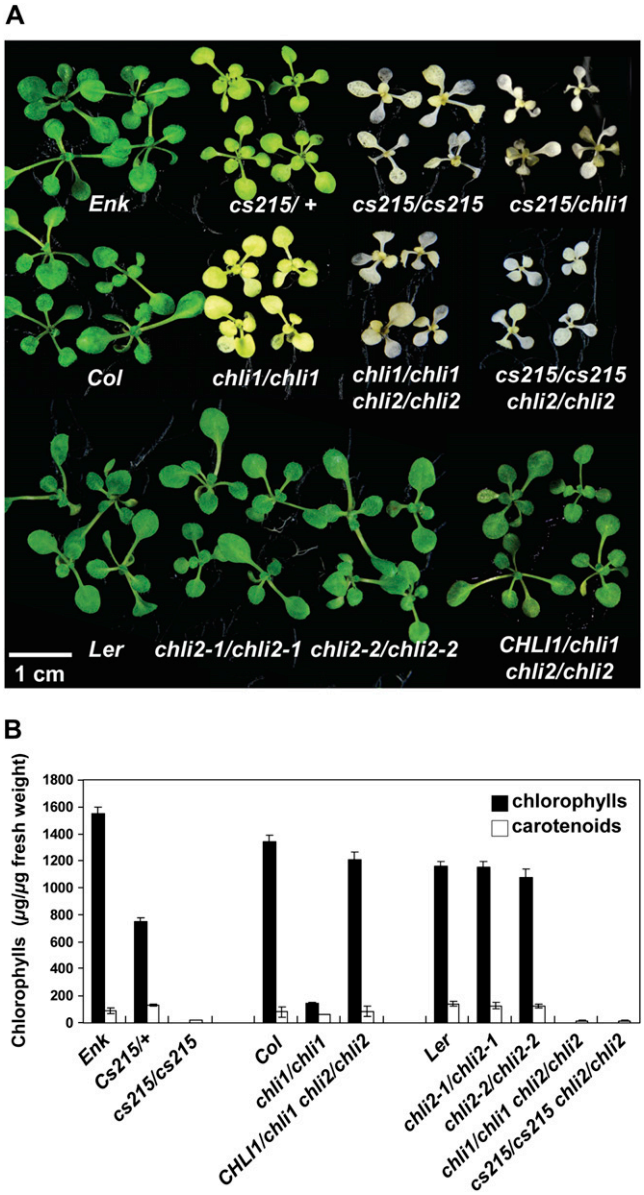

Figure 1. Phenotypes of various mutants and double mutants. A, Plants of the indicated genotypes were grown on MS medium for 12 d. B, Chlorophyll and carotenoid contents in 12-d-old plants as shown in A. Data shown are means ± SD from five independent samples per genotype, each sample containing five to eight plants.

and Methods"). Initial mapping placed the *cs215* locus between markers AG and SGCSNP43 on chromosome IV (Fig. 2A). Data from three recombinant plants delimited the *cs215* locus to the region encompassed by bacterial artificial chromosomes F28J12 and F28A21. One of the genes in this region, At4g18480 encoding CHLI1, has been shown to have mutant alleles with semidominant pale-green phenotypes (Kjemtrup et al., 1998; Fitzmaurice et al., 1999; Hansson et al., 2002; Soldatova et al., 2005). Therefore, we sequenced the region of At4g18480 from *cs215* and found that *cs215* indeed had a C-to-T mutation at nucleotide 584 that converted a Thr at residue 195 to an Ile (Fig. 2B). Pale-green plants were heterozygous at this position. Thr-195 is located between the Walker A and Walker B motifs of the ATPase domain of CHLI and is only 10 residues downstream from the mutations in the barley *Xan-h*^{clo161} and maize (*Zea mays*) *Oy1-N1989* mutants (Fig. 2B), both of which are semidominant alleles of the *chli* mutants. When a *cs215*/+ plant was crossed with a *chli1*-knockout mutant (see below), the F1 seedlings had the same phenotype as *cs215*/*cs215* (*cs215*/*chli1*; Fig. 1A), further supporting that *cs215* was allelic to *chli1*. We also sequenced the *CHLI2* gene from the Enk ecotype, and the result indicated that *CHLI2* from Enk has an identical deduced amino acid sequence to that of *CHLI2* from Col (data not shown). Therefore, it is unlikely that the severe phenotype of *cs215* was caused

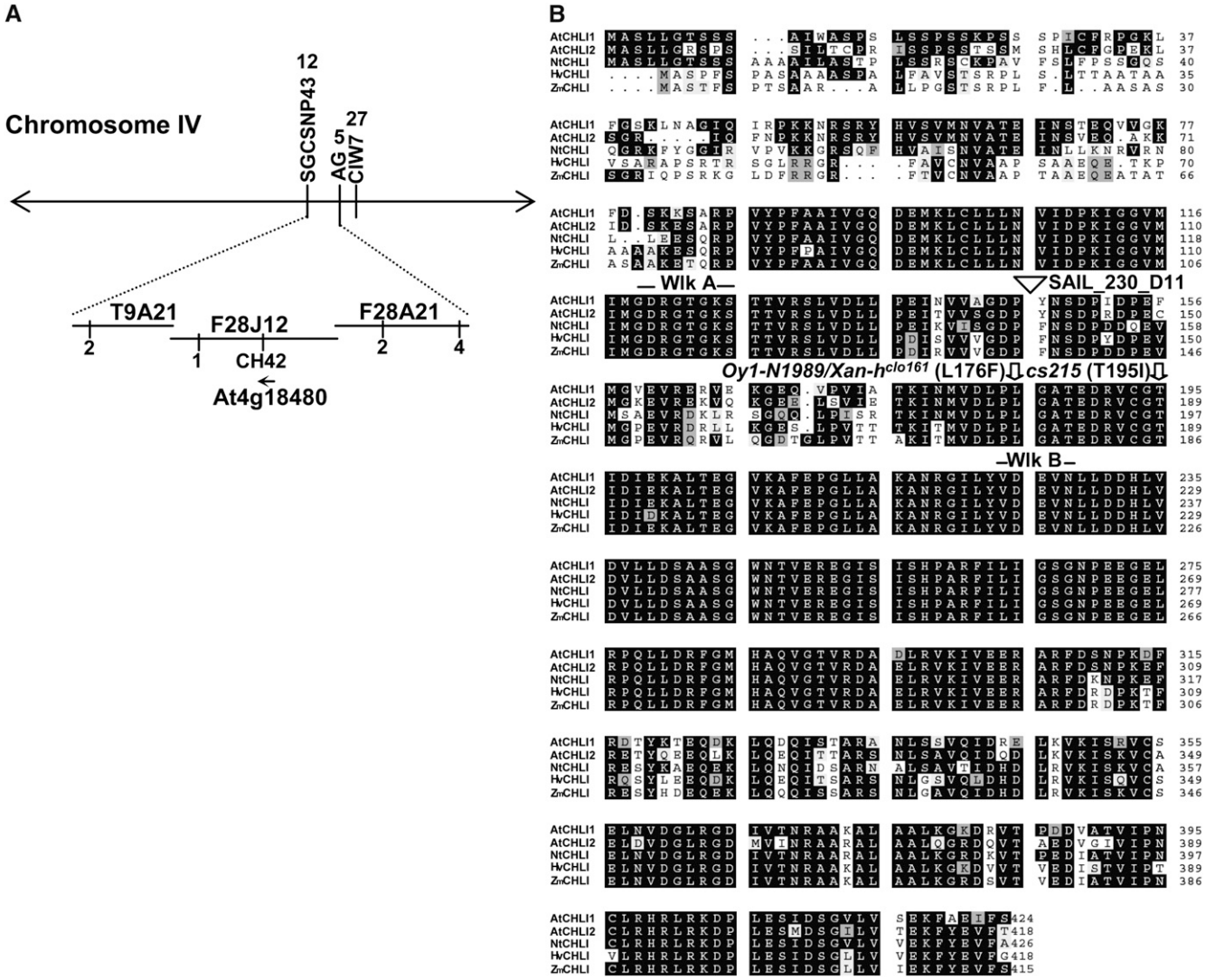

Figure 2. Identification of the *cs215* locus. A, Summary of *cs215* mapping. Vertical lines indicate the positions of PCR-based markers. Values beneath the lines indicate the number of recombinant plants. The direction of transcription of the At4g18480 open reading frame is indicated (arrow). B, Alignment of Arabidopsis CHLI1 and related proteins. Alignment of Arabidopsis CHLI1 (AtCHLI1) and CHLI2 (AtCHLI2), Sulfur from tobacco (*Nicotiana tabacum*; NtCHLI), and CHLI from barley (HvCHLI) and maize (ZmCHLI). Walker A (Wlk A) and Walker B (Wlk B) motifs of the ATP-binding fold are marked above the sequences. Mutation positions of the *chli1* (SAIL_230_D11), *cs215*, and maize *Oy1-N1989*/barley *Xan-h*^{clo161} mutants are also indicated.

by a synthetic effect with natural variations in the *CHLI2* gene of the Enk ecotype.

CHLI2 Supports Some Chlorophyll Biosynthesis in the Absence of CHLI1

To compare the phenotype of *c215* with those of other *chli1* mutants, a mutant line with a T-DNA insertion in the third exon of the *CHLI1* gene (SAIL_230_D11; Fig. 3A) was obtained from the ABRC. This mutant produced a truncated *CHLI1* mRNA but no full-length transcripts or transcripts behind the T-DNA insertion site (Fig. 3B, lanes 4–6). It was yellow in appearance (Fig. 1A) and had less than 10% of the wild-type level of chlorophylls (Fig. 1B), similar to the levels reported for other *chli1*-null mutants (Rissler et al., 2002). These data suggested that SAIL_230_D11 is most likely also a *chli1*-null mutant. SAIL_230_D11 will be referred to as the *chli1/chli1* mutant herein.

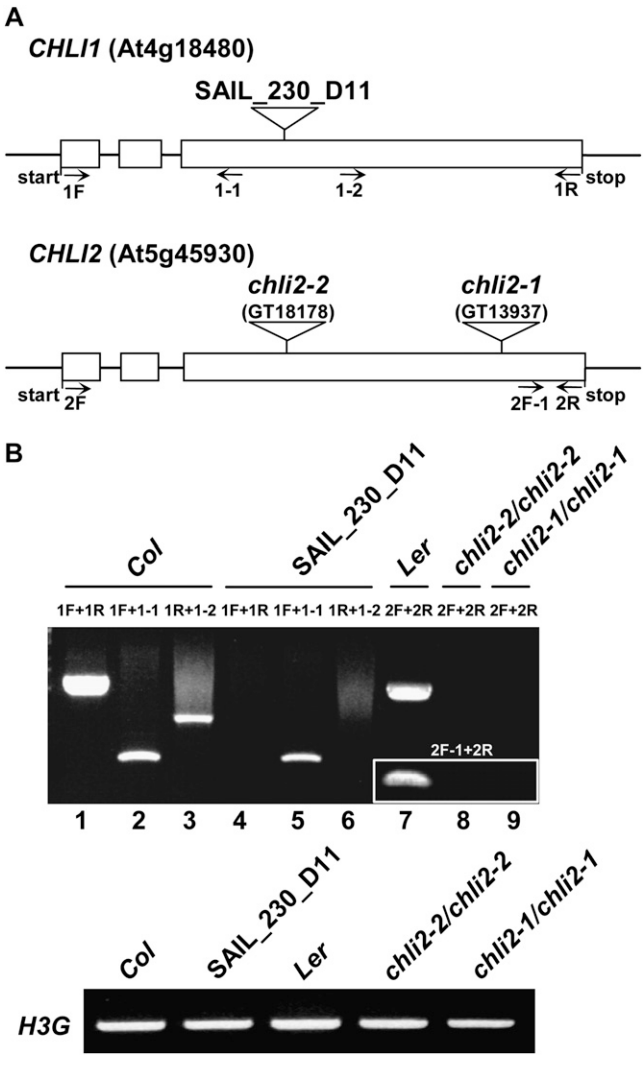

Figure 3. Transcript analyses of the *chli1/chli1* and *chli2/chli2* mutants. A, Schematic representation of the structures of the *CHLI* genes and the location of each insertion site. Exons are represented by white boxes, and introns are represented by lines between boxes. Location and direction of primers used for RT-PCR are also indicated (arrows). B, Analyses of *CHLI* transcripts in *chli1/chli1* and *chli2/chli2* mutants. Total RNA extracted from wild-type and mutant plants was analyzed by RT-PCR. *Histone 3G* (*H3G*; At4g40040) transcripts were analyzed as a control.

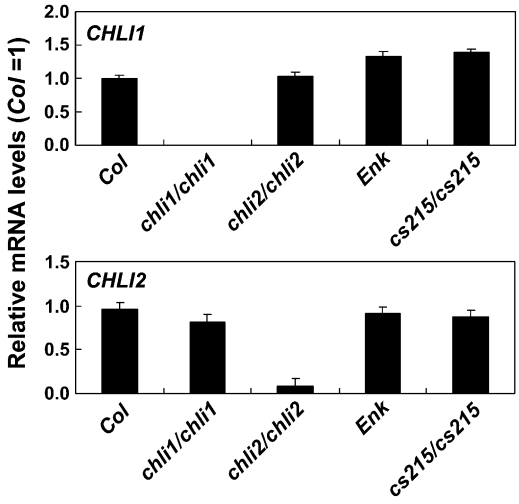

Figure 4. *CHLI1* and *CHLI2* mRNA levels in the wild type and *chli* mutants. Total RNA was isolated from 12-d-old seedlings. *CHLI1* and *CHLI2* mRNA levels were determined by real-time quantitative RT-PCR as described in "Materials and Methods." Data shown are means ± SD from four independent samples per genotype, and each sample contained five plants.

Comparison of *chli1/chli1* with *cs215/cs215* revealed that *chli1/chli1* had more chlorophylls than *cs215/cs215* (Fig. 1B). Arabidopsis has two genes encoding CHLI: *CHLI1* and *CHLI2*. It is possible that in the *chli1/chli1* mutant, *CHLI2* can still support some chlorophyll biosynthesis. In the *cs215/cs215* mutant, the presence of the cs215 mutant protein might prevent CHLI2 from functioning, resulting in the phenotype difference between *cs215/cs215* and *chli1/chli1*. To verify this, we obtained two mutant lines, GT13937 (Kobayashi et al., 2008) and GT18178, with Ds transposon insertion in the *CHLI2* gene (Fig. 3A). Reverse transcription (RT)-PCR analyses indicated that neither mutant produced any full-length *CHLI2* mRNA or any *CHLI2* mRNA 3′ to the Ds insertion site (Fig. 3B, lanes 8 and 9 and inset). Both mutants were wild type in appearance (Fig. 1A) and in chlorophyll levels (Fig. 1B). GT13937 and GT18178 are referred to herein as *chli2-1* and *chli2-2*, respectively.

We crossed *cs215/+* and *CHLI1/chli1* with *chli2-1/chli2-1* and *chli2-2/chli2-2* to generate various double mutants. Results from crosses to *chli2-1/chli2-1* and to *chli2-2/chli2-2* were identical, and data from *chli2-1* are presented unless specified. Double mutants of *chli1/chli1 chli2/chli2* were albino (Fig. 1A) with no detectable chlorophylls (Fig. 1B). Compared with the *chli1/chli1* single mutant, the albino phenotype of the double

mutant indicated that the CHLI2 protein must be stable enough to provide some Mg-chelatase activity even in the absence of CHLI1. Furthermore, double mutants of *cs215/cs215 chli2/chli2* were indistinguishable from the *cs215* single (*cs215/cs215 CHLI2/CHLI2*) mutant (Fig. 1). Therefore, it is likely that the presence of the cs215 mutant protein had prevented CHLI2 from functioning. This may be because the expression level of *CHLI1* is much higher than that of *CHLI2*, as shown previously by Matsumoto et al. (2004). In the *cs215* mutant, the high amount of cs215 mutant protein may out-compete the low amount of CHLI2 in assembly with CHLD. It is also possible that the expression levels of *CHLI1* and *CHLI2* were similar (Rissler et al., 2002; Apchelimov et al., 2007) and that the presence of the cs215 mutant protein inhibited the expression of *CHLI2* as suggested previously (Soldatova et al., 2005).

The Expression Level of *CHLI2* Is Much Lower Than That of *CHLI1* and Is Not Affected by Mutations in *CHLI1*

To clarify the role of CHLI2, we compared the expression levels of *CHLI1* and *CHLI2* using real-time quantitative RT-PCR. Amounts of *CHLI1* and *CHLI2* RNA were determined by comparing with standard curves generated from known quantities of *CHLI1* and *CHLI2* plasmid DNA. The results showed that in 14-d-old seedlings, the ratio of *CHLI1* to *CHLI2* RNA was 5.86 ± 1.31 ($n = 5$). This result agrees with the reported miniarray data (Matsumoto et al., 2004) and is also supported by data found in Genevestigator (expression value of 9,764 versus 2,121 in rosette leaves) and MPSS (928 versus 132 transcripts per million in 21-d-old leaves) databases. The level of *CHLI2* was not changed in the *chli1/chli1* or *cs215/cs215* mutants (Fig. 4, bottom), indicating that mutations in *CHLI1* did not affect the expression of *CHLI2*. The level of *CHLI1* was also not changed in the *chli2/chli2* or *cs215/cs215* mutants (Fig. 4, top).

CHLI2 Driven by the *CHLI1* Promoter Can Rescue the *chli1/chli1 chli2/chli2* Double Mutant

It has been suggested that CHLI2 is defective in hexameric ring assembly due to changes in its C terminus (Apchelimov et al., 2007). However, it has also been shown that CHLI2 is an active ATPase (Kobayashi et al., 2008). To test the function of CHLI2 in vivo, we fused the *CHLI2* gene behind a 2.1-kb *CHLI1* promoter fragment and used this transgene (referred to herein as *pCHLI1*::*CHLI2*) to complement the *chli1/chli1 chli2/chli2* double mutant. Transgenic plants with one copy of the *pCHLI1*::*CHLI2* transgene were referred to as the *pCHLI1*::*CHLI2* (*chli1/chli1 chli2/chli2*) plants. For fair comparison, these plants were compared with plants with only one endogenous copy of *CHLI1* (genotype *CHLI1/chli1 chli2/chli2* and referred to herein accordingly). Nonetheless, *CHLI1/chli1 chli2/chli2* plants were similar to wild-type plants in both appearance (Fig. 1A) and chlorophyll levels (Fig. 1B).

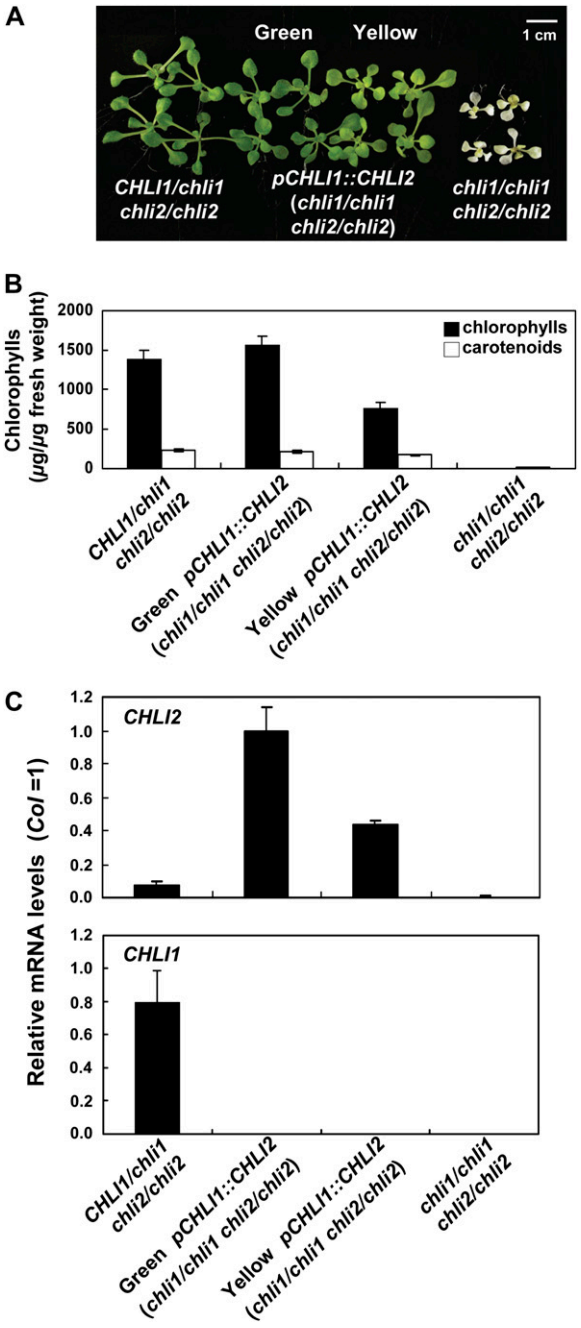

Figure 5. *CHLI2* driven by the *CHLI1* promoter rescued the *chli1/chli1 chli2/chli2* double mutant. A, Plants of the indicated genotypes were grown on MS medium for 12 d and then photographed. The *pCHLI1*::*CHLI2* (*chli1/chli1 chli2/chli2*) transgenic plants had phenotypes that ranged from fully green (Green) to slightly yellow in younger leaves (Yellow). Representative transgenic lines were photographed and used for analyses shown in B and C. B, Chlorophyll and carotenoid contents of 12-d-old plants as shown in A. Data shown are means ± SD derived from five independent samples per genotype, each sample containing five to eight plants. C, Comparison of *CHLI2* mRNA levels in the wild type and *chli* mutants. Seedlings were grown as described in A. mRNA levels were determined by real-time quantitative RT-PCR as described in "Materials and Methods." Data shown are means ± SD derived from five independent samples per genotype, each one containing five to eight plants. *CHLI1* transcript levels were also determined as controls.

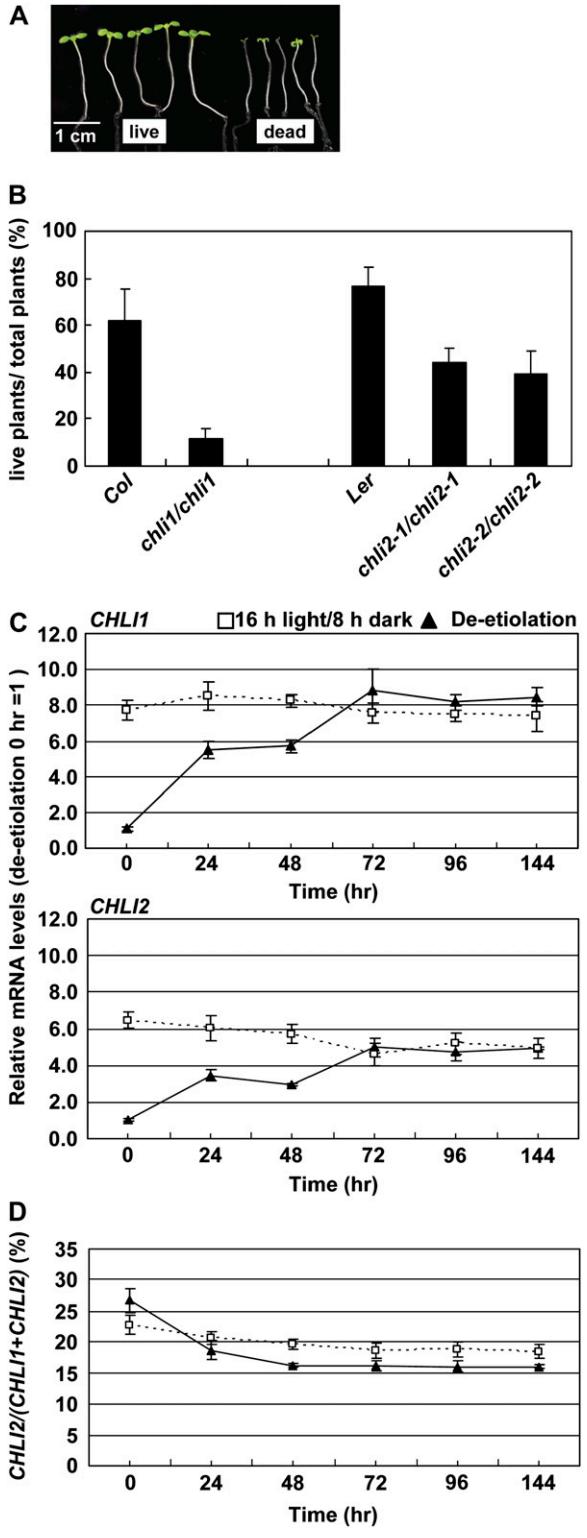

Figure 6. The *chli* mutants had lower survival rates during de-etiolation. Seeds were grown on MS medium and imbibed at 4°C in the dark for 3 d, exposed to light at 22°C for 1 d, and then moved to the dark to germinate at 22°C for 7 d. Etiolated seedlings were then transferred to a 16-h-light/8-h-dark cycle for another 6 d (de-etiolation) and then photographed. A, Examples of seedlings being scored as "live" or "dead." B, Seedling survival rates of Col, L*er*, *chli1/chli1*, *chli2-1/chli2-1*, and *chli2-2/chli2-2* after de-etiolation. Data shown are means ± SD of six independent experiments, each experiment containing 100 to 120 seedlings per genotype. C, Comparison of *CHLI1* and *CHLI2* mRNA levels in L*er* during de-etiolation (black triangles and solid lines). *CHLI1* and *CHLI2* mRNA levels were determined by real-time quantitative RT-PCR as described in "Materials and Methods." D, Percentage of *CHLI2* in total *CHLI* (*CHLI1*+*CHLI2*) during de-etiolation. Amounts of *CHLI1* and *CHLI2* mRNA were determined by real-time quantitative RT-PCR and deduced from standard curves produced from known quantities of *CHLI1* and *CHLI2* plasmid DNA. For both C and D, time on the *x* axis indicates hours after transferring to the 16-h-light/8-h-dark cycle after etiolation. Seedlings were harvested 3 h after light came on each day. Seedlings of the same age but grown under a 16-h-light/8-h-dark cycle since stratification were analyzed as a control (white squares and dotted lines). Data shown are means ± SD of four independent samples, each sample containing 50 to 60 plants. [See online article for color version of this figure.]

The *pCHLI1*::*CHLI2* (*chli1/chli1 chli2/chli2*) transgenic plants had phenotypes that ranged from fully green to slightly yellow in younger leaves (Fig. 5A, Green and Yellow, respectively). The Green transgenic plants had chlorophyll levels similar to those of *CHLI1/chli1 chli2/chli2* plants (Fig. 5B). This result indicated that *CHLI2* could substitute for *CHLI1* if expressed at a sufficient level. The Yellow transgenic plants had chlorophyll and *CHLI2* transcript levels about half of those in the Green transgenic plants (Fig. 5, B and C). This result further demonstrated that the expression level of *CHLI2* was correlated with the level of chlorophyll biosynthesis activity observed.

The *chli* Mutants Have Lower Survival Rates during De-Etiolation

To investigate if CHLI2 contributes to plant fitness, we compared the *chli* mutants with the wild type in de-etiolation experiments. Seeds were imbibed at 4°C in the dark for 3 d, exposed to light at 24°C for 1 d, and then moved to the dark to germinate at 24°C for 7 d. Etiolated seedlings were then transferred to a regular 16-h-light/8-h-dark cycle, and seedling survival rates were scored 6 d later. Seedlings that failed to expand their cotyledons (i.e. the two cotyledons had a combined length less than 0.25 cm) were scored as dead (Fig. 6A). As shown in Figure 6B, the *chli1/chli1* mutant had a 14% survival rate and the two alleles of *chli2/chli2* mutants had a 40% survival rate. Both rates were significantly lower than that of their corresponding wild type. This result suggested that both genes contributed to increase the seedling survival rate upon de-etiolation. We then analyzed the *CHLI1* and *CHLI2* RNA levels during de-etiolation, comparing with the *CHLI1* and *CHLI2* RNA levels in seedlings that were grown under a regular 16-h-light/8-h-dark cycle after cold stratification (Fig. 6C). The results indicated that the expression of both genes was induced by light upon de-etiolation. When the RNA levels of the two genes were directly compared, *CHLI1* was still severalfold higher than *CHLI2*, agreeing with the result that

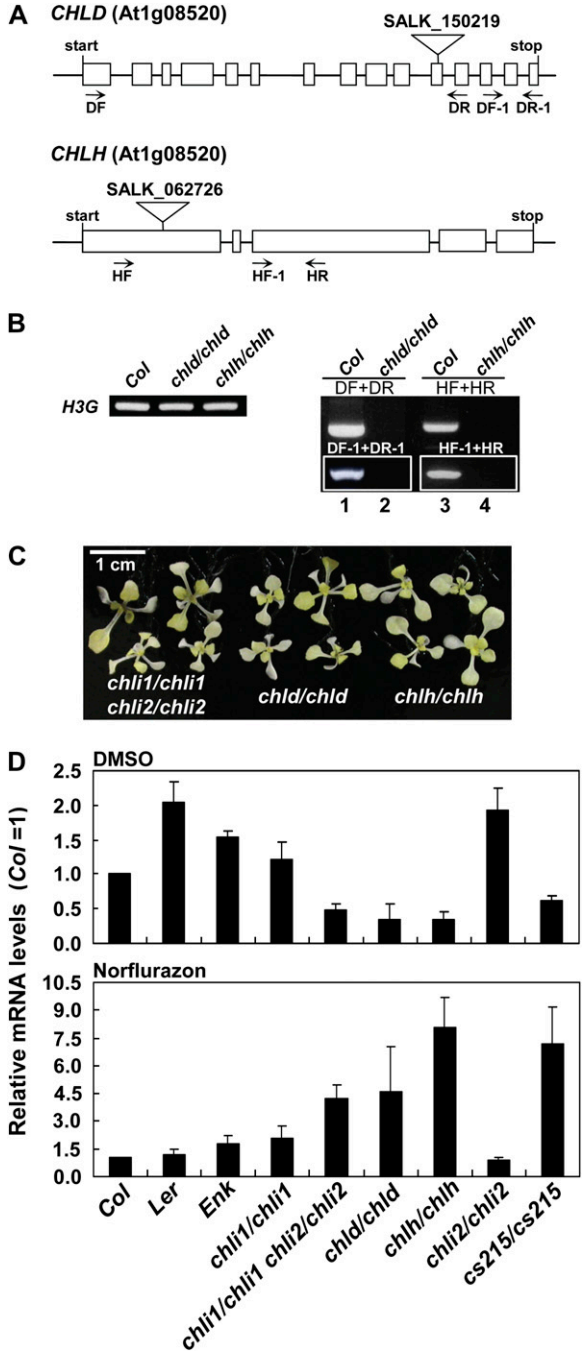

Figure 7. *Lhcb1* mRNA levels in Nf-treated wild type (Col, L*er*, and Enk), various *chli* mutants, and *chld/chld* and *chlh/chlh* mutants. A, Schematic representation of the *CHLD* and *CHLH* genes. Exons are represented by white boxes, and introns are represented by lines between the boxes. The locations of T-DNA insertion sites and RT-PCR primers are indicated. B, No transcript across the T-DNA insertion site or 3′ to the insertion site could be detected in the *chld/chld* or *chlh/chlh* mutants. Total RNA extracted from wild-type and mutant plants was analyzed by RT-PCR using primers indicated in A. *H3G* transcripts were analyzed as a control. C, Phenotypes of the *chli1/chli1 chli2/chli2*, *chld/chld*, and *chlh/chlh* mutants. Plants were grown on MS medium for 12 d. D, Comparison of *Lhcb1* mRNA levels in the wild type and mutants. Seedlings were grown on MS medium for 5 d. Homozygous pale-green or albino mutants (*chli1/chli1*, *cs215/cs215*, *chli1/chli1 chli2/chli2*, *chld/chld*, and *chlh/chlh*) were selected and, together with the *chli2/chli2* and wild-type seedlings, transferred to MS medium containing either 5 μM Nf or the same volume of dimethyl sulfoxide (DMSO). Seedlings were grown for another 5.5 d under strong continuous light (100 μmol m^{-2} s^{-1}) and then used for total RNA isolation. *Lhcb1* mRNA levels were determined by real-time quantitative RT-PCR as described in "Materials and Methods." Data shown are means ± SD derived from four independent samples per genotype, each sample containing 10 to 15 plants.

the survival rate of the *chli1* mutant was more severely affected than that of the *chli2* mutants. However, *CHLI2* contributed to about 27% of total *CHLI* RNA in the dark and only about 16% of total *CHLI* after de-etiolation (Fig. 6D), suggesting that *CHLI2* might have slightly more contribution in the dark. This might be the reason that *chli2* mutants had no clear phenotype when directly grown under the light but had a lower survival rate in transitions from dark to light.

The *chli1/chli1 chli2/chli2* Double Mutant and the *cs215/cs215* Mutant Are *gun* Mutants

Mutants in the H and D subunits of Mg-chelatase are *gun* mutants (Strand et al., 2003), but two alleles of the *chli1* mutants are not (Mochizuki et al., 2001). To investigate if the *chli1/chli1 chli2/chli2* double mutant or the *cs215/cs215* mutant would show the *gun* phenotype, we first obtained mutants with T-DNA insertion in the *CHLD* and *CHLH* genes for use as controls. The *chld* mutant allele was identical to the allele reported previously and has been shown to be a *gun* mutant (SALK_150219; Strand et al., 2003; Ankele et al., 2007). The *chlh* mutant has a T-DNA insertion in the first exon of the *CHLH* gene (SALK_062726; Fig. 7A). No transcripts across the T-DNA insertion site or 3′ to the T-DNA insertion site could be detected in either mutant (Fig. 7B), and both mutants had an albino phenotype similar to that of the *chli1/chli1 chli2/chli2* double mutant (Fig. 7C). We then measured *Lhcb1* transcript levels in these mutants after treatment with Nf. As shown in Figure 7D, the *chli1/chli1 chli2/chli2* double mutant accumulated a higher level of *Lhcb1* transcripts than the wild type, similar to the level found in the *chld/chld* mutant. Interestingly, *cs215/cs215* and *chlh/chlh* mutants accumulated an even higher level of *Lhcb1* transcripts. These results indicated that the *chli1/chli1 chli2/chli2* double mutant and the *cs215/cs215* mutant were *gun* mutants.

Absence of CHLI Causes Instability of CHLD

It has been shown that changes in the level of one Mg-chelatase subunit causes instability in other subunits (Hansson et al., 1999; Petersen et al., 1999). Therefore, we investigated whether the level of CHLD or CHLH proteins was affected in the various *chli* mutants. We used immunoblots to detect the levels

of the three Mg-chelatase subunits. As shown in Figure 8, in the *chli1/chli1* and *chli1/chli1 chli2/chli2* mutants, CHLI was reduced or absent and the amount of CHLD protein was also greatly reduced (lanes 4 and 6). In comparison, the *cs215/cs215* mutant still contained a normal amount of CHLI protein (Fig. 8, lane 7) and its amount of CHLD protein was also normal. On the other hand, the amount of CHLI was not affected by the *chld* mutation (Fig. 8, lane 8). These results agreed with results from barley showing that *chli*-null mutants also lacked CHLD but *chld* mutations did not affect the amount of CHLI (Petersen et al., 1999). Furthermore, the normal amount of CHLD in the *cs215* mutant suggested that the cs215 mutant protein could still complex with CHLD, agreeing with previous observations in barley that semidominant mutant chli protein could still complex with CHLD (Hansson et al., 1999). In addition, the presence of CHLD and CHLH in the *cs215/cs215* mutant also indicated that the *gun* phenotype of the *cs215/cs215* mutant was not caused by the absence of CHLD or CHLH. Interestingly, loss of CHLI or CHLD activity in the *chli1/chli1*, *chli1/chli1 chli2/chli2*, *cs215/cs215*, and *chld/chld* mutants seemed to have resulted in an increase of the CHLH protein level (Fig. 8, lanes 4 and 6–8).

DISCUSSION

The expression level of *CHLI2* was much lower than that of *CHLI1*. When driven by the *CHLI1* promoter, expression of *CHLI2* alone rescued the *chli1/chli1 chli2/chli2* double mutant. These data indicate that CHLI2 can be functionally equivalent to CHLI1 if expressed at a sufficient level. This result also agrees with results from Kobayashi et al. (2008) showing that CHLI2 is a functional ATPase. Previous proposals of CHLI2 rapid turnover and inability in hexameric ring assembly were based on data suggesting that *CHLI1* and *CHLI2* had similar expression levels (Rissler et al., 2002; Apchelimov et al., 2007), which might have resulted from probe or primer cross-reactions.

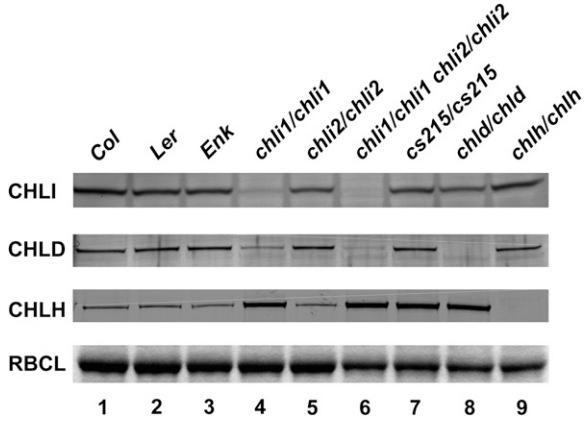

Figure 8. Immunoblot analyses of the three Mg-chelatase subunits in various mutants and corresponding wild types. Total proteins extracted from leaves of 14-d-old plants were analyzed by SDS-PAGE and immunoblots with antibodies against CHLI, CHLD, and CHLH. RBCL from the same set of samples as revealed by Coomassie Brilliant Blue staining was analyzed as a control.

The *chli2/chli2* mutants had no clear phenotype when grown in the light but had a lower survival rate during de-etiolation, suggesting that the presence of a second copy of *CHLI* may contribute to plant fitness under certain growth conditions. Although *CHLI1* was the major isoform in both light and dark, *CHLI2* contributed to about 27% of total *CHLI* RNA in the dark and only about 16% of total *CHLI* after de-etiolation. These results agreed with the mini-array data showing that *CHLI1* RNA was almost 3-fold of *CHLI2* in 3-week-old light-grown seedling but only 2-fold of *CHLI2* in 3-d-old etiolated seedlings (Matsumoto et al., 2004). These results suggest that the presence of CHLI2 may be more important in the dark or in a sudden dark-to-light transition as in the de-etiolation experiments. We searched several sequenced plant genomes and found that two copies of *CHLI* are present in *Chlamydomonas reinhardtii*, *Physcomitrella patens*, and *Populus trichocarpa* but only one copy is present in rice (*Oryza sativa*) and *Sorghum bicolor*. It is not clear why monocots seem to have lost the second copy of *CHLI*. It is possible that changes in the physiology of monocots rendered the second copy unnecessary.

It has been suggested that, because the N terminus of CHLD has some sequence similarity to CHLI, CHLD may interact with CHLH in the absence of CHLI and provide a low level of Mg-chelatase activity (Rissler et al., 2002). However, our data showed that both the *chli1/chli1 chli2/chli2* double mutant and the *cs215/cs215* mutant had no detectable chlorophylls and were indistinguishable from the *chld/chld*- and *chlh/chlh*-knockout mutants. In fact, similar to barley, the stability of CHLD seems to rely on the presence of CHLI. These results suggest that CHLD and CHLH support no significant chlorophyll biosynthesis in the absence of CHLI, agreeing with results from *Rhodobacter* and barley that all three subunits are required for the Mg-chelatase activity (Gibson et al., 1995; Willows et al., 1996; Kannangara et al., 1997).

We showed that the *chli1/chli1 chli2/chli2* double mutant and the *cs215/cs215* mutant showed the *gun* phenotype. Our data help remove doubts that knocking out the Mg-chelatase activity causes the *gun* phenotype. Indeed, mutants in all three subunits in barley have been shown to be *gun* mutants (Gadjieva et al., 2005). It has been shown recently that the immediate product of Mg-chelatase, Mg-protoporphyrin IX, does not accumulate under Nf treatment and therefore is unlikely to be the determinant for retrograde signaling (Mochizuki et al., 2008; Moulin et al., 2008). Therefore, it remains to be elucidated why perturbation of the tetrapyrrole biosynthesis pathway often causes the *gun* phenotype. It is also interesting that the *cs215/cs215* and the *chlh*-knockout mutants showed a higher level of

Lhcb1 accumulation than the *chli1/chli1 chli2/chli2* double mutant and the *chld/chld* mutant, even though they are indistinguishable in appearance. These mutants may be useful materials to facilitate the identification of compounds whose accumulation levels correlate with the *Lhcb1* transcript levels and that therefore may be candidates for the signaling molecules.

MATERIALS AND METHODS

Positional Cloning of the *cs215* Locus

The *cs215* mutant of Arabidopsis (*Arabidopsis thaliana*) is in the Enk ecotype. Heterozygous *cs215* plants were crossed with wild-type Col and L*er* plants. DNA from F2 seedlings with the *cs215/cs215* phenotype was isolated for mapping. Simple sequence length polymorphism and cleaved-amplified polymorphic sequence markers between the Col and L*er* ecotypes (http://www.Arabidopsis.org) were tested on Enk DNA to identify markers that could distinguish Enk versus Col or Enk versus L*er* ecotypes.

Plant Materials, Growth Conditions, and Treatments

The *cs215* (Enk ecotype) and *chli1*, *chld*, and *chlh* (Col ecotype) mutants were obtained from the ABRC (http://www.Arabidopsis.org/abrc/). The *chli2* mutants GT13937 and GT18178 (L*er* ecotype) were obtained from Cold Spring Harbor Laboratory (http://genetrap.cshl.org). The T-DNA or Ds insertion positions in the mutants were confirmed by PCR and direct sequencing of the PCR products (for primer sequences, see Supplemental Table S1). Mutants were backcrossed to their corresponding wild type, and lines with single T-DNA or Ds insertion were selected based on the kanamycin or BASTA (glufosinate ammonium) resistance segregation ratio.

Sterilized seeds were plated on Murashige and Skoog (MS) medium containing 0.3% Gelrite, 1× Murashige and Skoog salts, Gamborg's B5 vitamin, and 2% Suc. After a 3-d cold stratification, seeds were grown in growth chambers under a 16-h photoperiod with a light intensity of approximately 60 μmol m^{-2} s^{-1} at 22°C. Total chlorophyll and carotenoid contents were determined as described (Lichtenthaler, 1987). Kanamycin selection of T-DNA and Ds transposon-containing seedlings were performed on medium supplemented with kanamycin (Sigma-Aldrich) at 50 mg L^{-1}. The *pCHLI1*::*CHLI2* construct was obtained by two-step PCR (primers used were *Kpn*I-CHLI1F and *Kpn*I-CHLI2R for the first step and P1 and P2 for the second step), cloned into the transformation vector pPZP221 (Hajdukiewicz et al., 1994), transformed into *Agrobacterium tumefaciens* GV3101, and introduced into the *CHLI1/chli1 chli2/chli2* mutant using the floral spray method (Chung et al., 2000). Transgenic plants were screened on MS medium containing 100 mg L^{-1} G418.

For the *chli1/chli1* de-etiolation experiment, because the *chli1/chli1* mutant was sterile and could only be sown from seeds of *CHLI1/chli1* heterozygous plants, seeds from *CHLI1/chli1* heterozygous plants were first grown in the light to confirm the segregation ratio of the *chli1/chli1* mutant, which was almost always around 1:4. The same batch of seeds was then used for the de-etiolation experiments. When calculating survival rate, the theoretical number of *chli1/chli1* seedlings was deduced using the segregation ratio from light-grown seedlings. The number of survived *chli1/chli1* seedlings was then counted using the yellow cotyledons of the *chli1/chli1* mutant as an indication.

For Nf treatment experiments, seeds (from heterozygous plants of the albino and pale-green mutant lines and from homozygous plants of others) were sterilized and plated on MS medium. After a 3-d cold stratification, plates were moved to a growth chamber for 5 d. Albino (*cs215/cs215*, *chli1/chli1 chli2/chli2*, *chld/chld*, and *chlh/chlh*) and pale-green (*chli1/chli1*) mutants were selected and, together with *chli2-1/chli2-1* and wild-type seedlings, were transferred to new MS medium containing 5 μM Nf or the same volume of dimethyl sulfoxide and grown for another 5.5 d under strong continuous light (100 μmol m^{-2} s^{-1}).

RNA Analysis

Total RNA was isolated from Arabidopsis shoots with TRIzol reagent (Invitrogen) and treated with RQ1 RNase-Free DNase (Promega). Template cDNA was prepared using 1 μg of total RNA and the Moloney murine leukemia virus reverse transcription system (Promega). Real-time quantitative RT-PCR was performed using the LightCycler system (Roche Applied Science) and the Lightcycler-FastStart DNA Master SYBR Green I kit (Roche Diagnostics). Each PCR contained 10 to 50 ng of cDNA and 0.5 μM of each of the primer pairs. The initial denaturing step of 10 min was followed by 40 PCR cycles of 95°C for 10 s, 60°C for 5 s, and 72°C for 1 s per 25 bp of the expected product. After the PCR, the melting temperature was tested. Quantification was performed using LightCycler Relative Quantification software version 1.0. Normalization was done using the transcript level of *H3G* and confirmed by the transcript level of *ubiquitin10*.

Immunoblots

Total proteins from leaves of 14-d-old plants were extracted with SDS sample buffer (300 mM Tris-HCl, pH 8.5, 1 mM EDTA, pH 8.0, 8% SDS, and 1 mM phenylmethylsulfonyl fluoride). Forty micrograms of total proteins was separated by SDS-PAGE and transferred to Immobilon-P membrane (Millipore). Immunostaining was performed with antisera to soybean (*Glycine max*) CHLI and CHLH and *Plectonema boryanum* CHLD at a 1:1,000 dilution followed by secondary staining with an alkaline phosphatase-conjugated goat anti-rabbit serum at a 1:1,000 dilution. Colorimetric development with 5-bromo-4-chloro-3-indolyl phosphate and nitroblue tetrazolium was used to visualize protein bands.

Supplemental Data

The following materials are available in the online version of this article.

Supplemental Table S1. Primers used in this study.

ACKNOWLEDGMENTS

We thank Wei-Ning Hwang, Ming-D Yang, and Dr. Chi-Chou Chiu for initial mapping of the *cs215* locus. We thank the ABRC for the *cs215*, *chld*, and *chlh* mutants and Cold Spring Harbor Laboratory for the *chli2* mutants GT13937 and GT18178. We thank Dr. Tatsuru Masuda for providing the CHLI, CHLD, and CHLH antibodies. We thank Dr. Harry Wilson of Academia Sinica for English editing.

Received January 7, 2009; accepted April 6, 2009; published April 10, 2009.

LITERATURE CITED

Ankele E, Kindgren P, Pesquet E, Strand A (2007) In vivo visualization of Mg-protoporphyrin IX, a coordinator of photosynthetic gene expression in the nucleus and the chloroplast. Plant Cell **19:** 1964–1979

Apchelimov AA, Soldatova OP, Ezhova TA, Grimm B, Shestakov SV (2007) The analysis of the *ChlI 1* and *ChlI 2* genes using acifluorfen-resistant mutant of Arabidopsis thaliana. Planta **225:** 935–943

Brenner S, Johnson M, Bridgham J, Golda G, Lloyd D, Johnson D, Luo S, McCurdy S, Foy M, Ewan M, et al (2000) Gene expression analysis by massively parallel signature sequencing (MPSS) on microbead arrays. Nat Biotechnol **18:** 630–634

Chung MH, Chen MK, Pan SM (2000) Floral spray transformation can efficiently generate Arabidopsis transgenic plants. Transgenic Res **9:** 471–476

Cottage AJ, Mott EK, Wang JH, Sullivan JA, MacLean D, Tran L, Choy MK, Newell C, Kavanagh TA, Aspinall S, et al (2008) *GUN1* (*GENOMES UNCOUPLED1*) encodes a pentatricopeptide repeat (PPR) protein involved in plastid protein synthesis-responsive retrograde signaling to the nucleus. *In* J Allen, E Gantt, J Golbeck, B Osmond, eds, Photosynthesis: Energy from the Sun. 14th International Congress on Photosynthesis. Springer, Dordrecht, The Netherlands, pp 1201–1205

Fitzmaurice WP, Nguyen LV, Wernsman EA, Thompson WF, Conkling MA (1999) Transposon tagging of the sulfur gene of tobacco using engineered maize Ac/Ds elements. Genetics **153:** 1919–1928

Gadjieva R, Axelsson E, Olsson U, Hansson M (2005) Analysis of *gun* phenotype in barley magnesium chelatase and Mg-protoporphyrin IX monomethyl ester cyclase mutants. Plant Physiol Biochem **43:** 901–908

Gibson LC, Willows RD, Kannangara CG, von Wettstein D, Hunter CN (1995) Magnesium-protoporphyrin chelatase of *Rhodobacter sphaeroides*: reconstitution of activity by combining the products of the *bchH*, *-I*, and *-D* genes expressed in *Escherichia coli*. Proc Natl Acad Sci USA **92:** 1941–1944

Hajdukiewicz P, Svab Z, Maliga P (1994) The small, versatile *pPZP* family of *Agrobacterium* binary vectors for plant transformation. Plant Mol Biol **25:** 989–994

Hansson A, Kannangara CG, von Wettstein D, Hansson M (1999) Molecular basis for semidominance of missense mutations in the XANTHA-H (42-kDa) subunit of magnesium chelatase. Proc Natl Acad Sci USA **96:** 1744–1749

Hansson A, Willows RD, Roberts TH, Hansson M (2002) Three semidominant barley mutants with single amino acid substitutions in the smallest magnesium chelatase subunit form defective AAA+ hexamers. Proc Natl Acad Sci USA **99:** 13944–13949

Kannangara CG, Vothknecht UC, Hansson M, von Wettstein D (1997) Magnesium chelatase: association with ribosomes and mutant complementation studies identify barley subunit Xantha-G as a functional counterpart of *Rhodobacter* subunit BchD. Mol Gen Genet **254:** 85–92

Kjemtrup S, Sampson KS, Peele CG, Nguyen LV, Conkling MA, Thompson WF, Robertson D (1998) Gene silencing from plant DNA carried by a geminivirus. Plant J **14:** 91–100

Kobayashi K, Mochizuki N, Yoshimura N, Motohashi K, Hisabori T, Masuda T (2008) Functional analysis of *Arabidopsis thaliana* isoforms of the Mg-chelatase CHLI subunit. Photochem Photobiol Sci **7:** 1188–1195

Larkin R, Alonso J, Ecker J, Chory J (2003) GUN4, a regulator of chlorophyll synthesis and intracellular signaling. Science **299:** 902–906

Lichtenthaler H (1987) Chlorophylls and carotenoids: pigments of photosynthetic biomembranes. Methods Enzymol **148:** 350–382

Matsumoto F, Obayashi T, Sasaki-Sekimoto Y, Ohta H, Takamiya K, Masuda T (2004) Gene expression profiling of the tetrapyrrole metabolic pathway in Arabidopsis with a mini-array system. Plant Physiol **135:** 2379–2391

Mochizuki N, Brusslan JA, Larkin R, Nagatani A, Chory J (2001) *Arabidopsis genomes uncoupled 5* (GUN5) mutant reveals the involvement of Mg-chelatase H subunit in plastid-to-nucleus signal transduction. Proc Natl Acad Sci USA **98:** 2053–2058

Mochizuki N, Tanaka R, Tanaka A, Masuda T, Nagatani A (2008) The steady-state level of Mg-protoporphyrin IX is not a determinant of plastid-to-nucleus signaling in *Arabidopsis*. Proc Natl Acad Sci USA **105:** 15184–15189

Moulin M, McCormac A, Terry M, Smith A (2008) Tetrapyrrole profiling in *Arabidopsis* seedlings reveals that retrograde plastid nuclear signaling is not due to Mg-protoporphyrin IX accumulation. Proc Natl Acad Sci USA **105:** 15178–15183

Nott A, Jung HS, Koussevitzky S, Chory J (2006) Plastid-to-nucleus retrograde signaling. Annu Rev Plant Biol **57:** 739–759

Petersen BL, Møller MG, Jensen PE, Henningsen KW (1999) Identification of the *Xan-g* gene and expression of the Mg-chelatase encoding genes *Xan-f*, *-g* and *-h* in mutant and wild type barley (*Hordeum vulgare* L.). Hereditas **131:** 165–170

Rissler HM, Collakova E, DellaPenna D, Whelan J, Pogson BJ (2002) Chlorophyll biosynthesis: expression of a second *chl I* gene of magnesium chelatase in Arabidopsis supports only limited chlorophyll synthesis. Plant Physiol **128:** 770–779

Soldatova O, Apchelimov A, Radukina N, Ezhova T, Shestakov S, Ziemann V, Hedtke B, Grimm B (2005) An *Arabidopsis* mutant that is resistant to the protoporphyrinogen oxidase inhibitor acifluorfen shows regulatory changes in tetrapyrrole biosynthesis. Mol Genet Genomics **273:** 311–318

Strand A, Asami T, Alonso J, Ecker JR, Chory J (2003) Chloroplast to nucleus communication triggered by accumulation of Mg-protoporphyrinIX. Nature **421:** 79–83

Susek R, Ausubel F, Chory J (1993) Signal transduction mutants of Arabidopsis uncouple nuclear *CAB* and *RBCS* gene expression from chloroplast development. Cell **10:** 787–799

Willows RD, Gibson LC, Kanangara CG, Hunter CN, von Wettstein D (1996) Three separate proteins constitute the magnesium chelatase of *Rhodobacter sphaeroides*. Eur J Biochem **235:** 438–443

Zimmermann P, Hirsch-Hoffmann M, Hennig L, Gruissem W (2004) GENEVESTIGATOR: Arabidopsis microarray database and analysis toolbox. Plant Physiol **136:** 2621–2632